TRENDS IN SCIENCES 2025; 22(8): 10089
https://doi.org/10.48048/tis.2025.10089
RESEARCH ARTICLE

Determination of Mercury Ions Level in River Water Using an Arduino Uno-Based TCS3200 Color Sensor with Silver Nanoparticle Indicators Synthesized from *Moringa Oleifera* Leaf Extract

Khairi Suhud[1,*], Sri Rahayu Ningsih[1], Muhammad Syukri Surbakti[2], Muhammad Daffa Hadistya[1], Sitti Saleha[1], Yusnaidar[3], Siti Aishah Hasbullah[4], Ahmad Fairuz Bin Omar[5], Fathurrahmi[1], Muhammad Rifki Fauzan Damanik[6] and Andriy Anta Kacaribu[7]

[1]*Department of Chemistry, Faculty of Mathematics and Natural Science, Universitas Syiah Kuala, Banda Aceh 23111, Indonesia*
[2]*Department of Physics, Faculty of Mathematics and Natural Science, Universitas Syiah Kuala, Banda Aceh 23111, Indonesia*
[3]*Department of Chemistry, Faculty of Science and Technology, Universitas Jambi, Jambi 36361, Indonesia*
[4]*Department of Chemistry, Faculty of Science Technology, Universiti Kebangsaan Malaysia, Selangor 43600, Malaysia*
[5]*School of Physics, Universiti Sains Malaysia, USM Penang 11800, Malaysia*
[6]*Department of Biology Education, Faculty of Teacher Training and Education, Universitas Syiah Kuala, Banda Aceh 23111, Indonesia*
[7]*Doctoral Program of Agricultural Science, Postgraduate School, Universitas Syiah Kuala, Banda Aceh 23111, Indonesia*

([*]Corresponding author's e-mail: khairi@usk.ac.id)

Received: 4 March 2025, Revised: 7 April 2025, Accepted: 14 April 2025, Published: 20 June 2025

Abstract

Mercury ions (Hg^{2+}) are highly toxic due to their neurotoxic properties. They pose significant risks to organisms and humans, especially when they accumulate in the body and frequently contaminate water. An Arduino Uno-based TCS3200 color sensor utilizing silver nanoparticles (AgNPs) as indicators offer a promising alternative for detecting Hg^{2+}. This approach is characterized by its simplicity, cost-effectiveness, environmental friendliness, and effectiveness for real-time detection in resource-limited areas. This study synthesized AgNPs from the ethyl acetate extract of *Moringa oleifera* leaves. These AgNPs were tested for selectivity against various metals commonly found in aquatic environments. Once the selective metals were identified, sensitivity and selectivity tests were conducted to confirm that the sensor accurately measures specific analytes, even in the presence of other components within a sample. The results showed that the synthesized AgNPs are highly selective and specific for Hg^{2+} ions, achieving an accuracy range of 89.3 - 110 %. The sensor can detect Hg^{2+} ions with a detection limit (DL) of 0.069 ppm. Analysis of river water samples revealed Hg^{2+} concentrations ranging from 0.128 to 0.287 ppm. Hg^{2+} concentration was measured using a TCS3200 color sensor and validated against UV-Vis spectrophotometry. This confirmed its comparable results and effectiveness for accurate Hg^{2+} detection in real-world water samples and resource-limited areas.

Keywords: Silver nanoparticles, Color sensor TCS3200, Arduino uno, Mercury ions, *Moringa oleifera* leaf extract, River water, Environmental monitoring

Introduction

Mercury (II) ions or Hg^{2+} is a prevalent toxic heavy metal that poses significant risks to human health and the environment [1]. It is persistent in the environment and can exist in metallic, inorganic, and organic forms [2]. Mercury ions can contaminate water and spread through the food chain, ultimately disrupting human bodily processes by causing kidney failure, nervous system damage, and cardiovascular issues [3]. Mercury is one of the most toxic metal pollutants impacting environmental and human health [4]. Mercury ions is released into the environment through activities such as mining, gasoline refining, and coal combustion, leading to water and soil contamination [5]. Due to its high toxicity, even at very low concentrations, mercury ions can accumulate in the body, causing severe functional impairments and irreversible damage to vital organs, including the brain and spinal cord [6,7]. Chronic exposure to low doses of mercury ions poses additional ecological risks and neurobehavioral effects, particularly in children, and is associated with cognitive impairments and other neurological deficits [8-10]. The World Health Organization (WHO) and the European Union (EU) have set the maximum allowable concentration of mercury ions in drinking water at 1 ppb (4.98 nM). In comparison, the US Environmental Protection Agency (EPA) sets this limit at 2 ppb (9.97 nM) [11,12].

Various techniques are available for detecting heavy metal ions, such as Hg^{2+}, including atomic absorption spectrometry (AAS) [13,14], microwave plasma atomic emission spectroscopy (MP-AES) [15,16], and inductively coupled plasma mass spectrometry (ICP-MS) [17-19]. Although these methods offer high sensitivity, they are often expensive, require complex equipment, and demand skilled personnel. Therefore, there is a need for new detection methods that are simpler, faster, and more cost-effective. Colorimetric sensors using nanoparticles as probes have shown promise as they allow for easy observation, low cost, and more straightforward operational procedures. Moreover, this approach offers excellent selectivity and sensitivity and it is environmentally friendly, posing no adverse environmental impacts [11,20-22].

The development of various colorimetric sensors using AgNPs for detecting mercury ions has been extensively explored. Typically, chemical reduction methods synthesize AgNPs using chemical agents as stabilizers and reducers. However, these methods can negatively impact environmental and health [23,24].

Green synthesis methods have recently been employed to synthesize AgNPs using plant extracts as reducing and stabilizing agents [25,26]. Memon *et al.* [27] utilized the leaves of the Jujube plant (*Ziziphus mauritiana*) as bioreductors in synthesizing AgNPs. This plant contains secondary metabolites such as flavonoids, ascorbic acid (vitamin C), phenolic acids, and minerals [27]. Similar research has been conducted on the biosynthesis of AgNPs from onion extract as a colorimetric indicator for heavy metals [22]. According to Mehwish *et al.* [28], the formation of AgNPs likely involves polyphenol or flavonoid compounds with hydroxyl (-OH) functional groups capable of reducing Ag^{+} ions to Ag^{0} in the form of AgNPs [28]. Mohammed *et al.* [29] also described the formation of AgNPs as indicated by a color change in the solution from pale yellow to dark reddish-brown.

Moringa oleifera, commonly known as *Moringa*, is a medicinal plant native to India, predominantly found in Southern India and Southeast Asia [30]. *Moringa* leaves are renowned for their extensive health benefits and are frequently utilized in traditional medicine. They are known to act as stimulants for blood circulation and the heart, as well as possessing antitumor, antiepileptic, anti-ulcer, anti-inflammatory, antispasmodic, antihypertensive, diuretic, antidiabetic, hepatoprotective, antioxidant, antifungal, and antibacterial properties [31-33]. The leaves of *Moringa* are rich in proteins, carbohydrates, phenols, vitamins, kaempferol, potassium, calcium, and amino acids [28]. Additionally, they contain compounds such as ascorbic acid, polyphenols, flavonoids, glycosides, and carotenoids [34].

This study synthesized AgNPs via a green synthesis method using *Moringa* leaf extract as a colorimetric indicator, for determining mercury ions concentrations in river water samples. The TCS 3200 color sensor was employed for this analysis. The TCS 3200 has been widely utilized in the study of various types of samples, such as tartrazine [35], rhodamine B [36], borax [37], capsaicin in sauces [38], and mercury ions [39,40]. Integrating the TCS 3200 color sensor with AgNPs synthesized from *Moringa oleifera* leaf extract

offers a promising approach for detecting mercury ions in river water. The green synthesis method provides an eco-friendly alternative for producing AgNPs, while the colorimetric response enables efficient and accurate detection. Combined with Arduino Uno-based control, this method represents a low-cost, accessible solution for environmental monitoring of mercury ions contamination, addressing the need for practical and scalable technologies in water quality.

Materials and methods

Materials and equipment

The materials used in this study included *Moringa* leaves obtained from the Limpok Village, Aceh Besar Regency, Indonesia. River water samples were collected from Alur Mas River, South Aceh Regency, Indonesia, as a site for gold extraction activities, and described as previous studies [40,41]. Chemicals used were $AgNO_3$, C_2H_5OH, $CH_3COOC_2H_5$, Na_2CO_3, quercetin, $AlCl_3$, CH_3COOK, $FeCl_3$, $CaCl_2$, $FeCl_2{\cdot}4H_2O$, NaCl, $Pb(NO_3)_2$, $Co(NO_3)_2{\cdot}6H_2O$, $CuSO_4{\cdot}5H_2O$, $ZnCl_2$, $HgCl_2$, HCl, Folin-Ciocalteu reagent, magnesium powder (were analytical grade purchased from Merck and Sigma Aldrich, Jakarta Indonesia) and deionized water. The equipment utilized in the research included a UV-Vis Spectrophotometer (Thermo Scientific), FTIR (Thermo Scientific), TEM (TEM HT7700), TCS3200 Color Sensor (ICTAOS/AMS), and Arduino Uno (Wavgat).

Hardware and software preparation

The hardware setup began with the design of a block diagram consisting of input, processing, and output components, as illustrated in **Figures 1(A) - 1(C)**. The input component is the TCS3200 color sensor, the processing component is the Arduino Uno microcontroller, and the output component is a personal computer (PC) or laptop, which serves as the data storage workstation for the color sensor's detections. The TCS3200 color sensor, acting as the input block, is connected to the Arduino Uno, the processing block, by linking the sensor's pins to the corresponding pins on the Arduino Uno using Arduino jumper cables [36], as demonstrated in **Figure 1(D)**. The software preparation aims to acquire RGB data displayed on a laptop or computer screen. The software used to enable the Arduino Uno to store data is the Arduino Integrated Development Environment (IDE). In this study, programming and code development were carried out using Arduino Uno IDE version 1.8.14, available for free download from the official website.

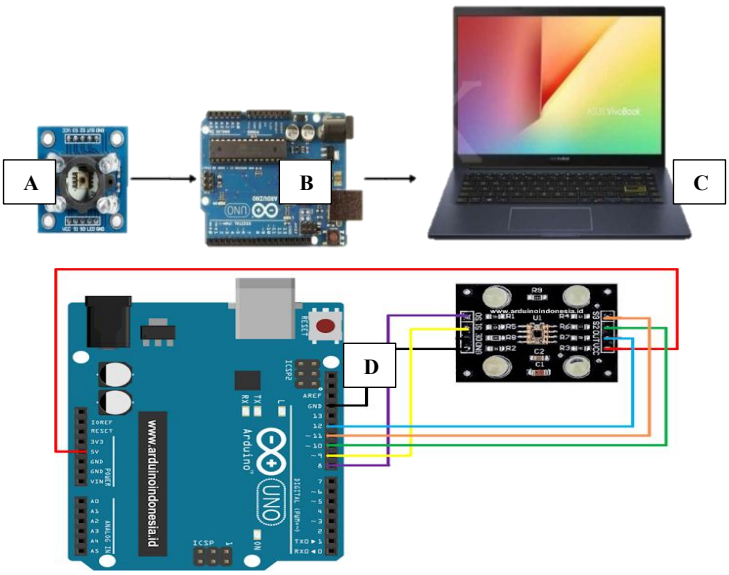

Figure 1 Hardware preparation block diagram (A) TCS3200 color sensor as an input; (B) Arduino Uno as a process; and (C) PC/Laptop as detector to read the output; (D) schematic diagram of the TCS3200 color sensor using Arduino Uno [36].

Preparation of *Moringa* leaf extract

Moringa leaves were cleaned and air-dried at room temperature (25 °C). A total of 203.886 g of dried *Moringa oleifera* leaves were subjected to maceration using ethanol as the extraction solvent for 2×24 h^2, with the process repeated 4 - 5 times to ensure thorough extraction of bioactive compounds. The resulting extract was then filtered and concentrated using a rotary evaporator to remove ethanol, yielding a crude ethanol extract. To further fractionate the bioactive components, the ethanol extract was partitioned using ethyl acetate, a moderately polar solvent, to selectively extract compounds with different solubility properties. This partitioning process was repeated 3 - 4 times to maximize separation efficiency. The ethyl acetate fraction was then concentrated using a rotary evaporator to obtain a thick ethyl acetate extract, following the method described by Ogundipe *et al.* [42] with modifications.

Qualitative tests for phenolics and flavonoids

The qualitative test for phenolics was conducted by adding 2 drops of 5 % $FeCl_3$ solution to 1 mL of *Moringa* leaf extract. A dark green color indicates the presence of phenolic compounds [43]. The qualitative test for flavonoids involved adding 0.5 g of magnesium powder and 1 mL of concentrated HCl to 1 mL of *Moringa* leaf extract, then shaking and observing the mixture. The appearance of a pink or red color indicates the presence of flavonoids [44].

Quantitative tests for phenolics and flavonoids

Total phenolic content (TPC) testing

The testing began with the preparation of a standard solution for gallic acid. A total of 50 mg of gallic acid was weighed and dissolved in 1 mL of ethanol, then diluted to a final volume of 50 mL with distilled water, yielding a 1,000 ppm gallic acid stock solution. This stock solution prepared a series of concentrations- 100, 125, 150, 175 and 200 ppm-. For each concentration, 0.2 mL was taken and mixed with 15.8 mL of distilled water and 1 mL of Folin-Ciocalteu reagent and then homogenized by shaking. The mixture was left to stand for 8 min, after which 3 mL of 10 % Na_2CO_3 solution was added to each and shaken until homogenized. The mixtures were then allowed to stand for 2 h at room temperature. Absorbance measurements were performed using a UV-Vis spectrophotometer at a maximum wavelength of 765 nm. A gallic acid standard solution calibration curve was constructed to obtain the linear regression equation.

The total phenolic content was determined using the Folin-Ciocalteu method with gallic acid as the standard solution. 100 mg of ethanol and ethyl acetate extracts from *Moringa* leaves were dissolved in distilled water to a volume of 10 mL. Each solution was then diluted with distilled water to achieve a concentration of 1,000 ppm. Subsequently, 0.2 mL of each extract solution was pipetted and mixed with 15.8 mL of distilled water and 1 mL of Folin-Ciocalteu reagent, followed by shaking until homogeneous. The mixtures were allowed to stand for 8 min and then 3 mL of 10 % Na_2CO_3 solution was added to each, followed by shaking until homogeneous. The mixtures were left to stand for 2 h at room temperature. Absorbance was measured using a UV-Vis spectrophotometer at a maximum wavelength of 765 nm, with 3 repetitions. The average absorbance values were substituted into the linear regression equation of the gallic acid standard to determine the total phenolic content in the ethanol and ethyl acetate extracts of *Moringa* leaves [45,46].

Total flavonoid content (TFC) testing

The quantitative assessment of TFC began with preparing a quercetin standard solution. A total of 25 mg of quercetin was weighed and dissolved in 25 mL of ethanol to create a 1,000 ppm quercetin stock solution. From this stock solution, 1 mL was pipetted and diluted with ethanol to a total volume of 10 mL, resulting in a 100-ppm quercetin standard solution. From this 100-ppm standard, a series of concentrations-2, 4, 6, 8 and 10 ppm-was prepared. Each concentration was taken as 1 mL and mixed with 3 mL of ethanol, 0.2 mL of $AlCl_3$, 0.2 mL of 1 M potassium acetate, and 5.6 mL of distilled water. The solutions were then incubated for 30 min at room temperature, and their absorbance was measured using a UV-Vis spectrophotometer at a wavelength of 440 nm, with 3 repetitions. A calibration curve for the quercetin standard solution was constructed to obtain the linear regression equation.

The total flavonoid content was determined using $AlCl_3$ with quercetin as the standard solution. 25 mg of ethanol and ethyl acetate extracts from *Moringa* leaves were dissolved in 25 mL of ethanol to produce 1,000

ppm extract solutions. Each extract solution was pipetted as 5 mL and diluted with ethanol to a total volume of 50 mL, resulting in 100 ppm extract solutions. From each extract solution, 1 mL was mixed with 3 mL of ethanol, 0.2 mL of $AlCl_3$, 0.2 mL of 1 M potassium acetate, and 5.6 mL of distilled water. The mixtures were incubated for 30 min at room temperature, and absorbance was measured using a UV-Vis spectrophotometer at a wavelength of 440 nm, with 3 repetitions. The average absorbance values were substituted into the linear regression equation of the quercetin standard to determine the total flavonoid content in the ethanol and ethyl acetate extracts of *Moringa* leaves [45,46].

Synthesis of AgNPs

To synthesize silver nanoparticles (AgNPs), 20 mL of *Moringa* leaf ethyl acetate extract was mixed with 180 mL of 1 mM $AgNO_3$ solution in a 250 mL volumetric flask. The mixture was heated to 70 °C and stirred using a magnetic stirrer at 250 rpm for 90 min. The resulting color change to yellowish-brown indicated the formation of AgNPs. Absorbance was measured using a UV-Vis spectrophotometer in the 380 - 500 nm wavelength range. The synthesized AgNPs were characterized using FTIR and TEM [47,48].

Detection of Hg^{2+} metal ions

Calibration curve preparation

Two mL of the synthesized silver nanoparticle solution was placed into vials, and 1 mL of Hg^{2+} standard solution (from $HgNO_3$ solutions) at concentrations of 0.1, 0.2, 0.3, 0.4 and 0.5 ppm was added to each vial. The RGB values were measured using the TCS3200 color sensor as the proposed method, and absorbance was measured using a UV-Vis spectrophotometer at the maximum wavelength as the standard method.

Determination of Hg^{2+} metal ions concentration

One mL of the prepared river water sample was mixed with 2 mL of the silver nanoparticle solution. The proposed method measured the RGB values using the TCS3200 color sensor, and the standard method measured absorbance using a UV-Vis spectrophotometer at the maximum wavelength.

Selectivity analysis

Selectivity testing was analyzed to determine the analytical error of chemical measurement [49]. The test aimed to determine which metal ions the synthesized AgNPs selectively detect. This test was conducted using 8 different metals: Ca^{2+}, Fe^{2+}, Na^{+}, Pb^{2+}, Co^{2+}, Cu^{2+}, Zn^{2+}, and Hg^{2+}, each at a concentration of 0.5 ppm. One mL of each 0.5 ppm metal standard solution was added to vials containing 2 mL of the silver nanoparticle solution. Color changes were observed, and absorbance was measured using a UV-Vis spectrophotometer, with RGB values measured by the TCS3200 color sensor as the proposed method.

Specificity analysis

Specificity testing aims to evaluate the ability of a reagent to accurately and selectively measure a particular analyte in the presence of other potential components in a sample. Specificity was determined by adding 2 mL of AgNPs to each vial, followed by 1 mL of 0.5 ppm Hg^{2+} metal solution. Subsequently, standard metal solutions of Ca^{2+}, Fe^{2+}, Na^{+}, Pb^{2+}, Co^{2+}, Cu^{2+} and Zn^{2+} concentrations of 0, 0.1, 0.3 and 0.5 ppm were added in volumes of 0.1 mL to each solution. Color changes were observed, and absorbance was measured using a UV-Vis spectrophotometer, with RGB values measured by the TCS3200 color sensor as the proposed method.

Sensitivity

Sensitivity was conducted to determine the detection capability and minimum concentration of Hg^{2+} that the AgNPs can detect. Sensitivity was evaluated by observing color changes in AgNPs mixed with standard Hg^{2+} solutions and comparing these with a blank solution (without Hg^{2+} addition) and through UV-Vis spectrophotometer analysis. Two mL of silver nanoparticle solution was placed in each vial and 1 mL of Hg^{2+} standard solution at concentrations of 0, 0.1, 0.2, 0.3, 0.4 and 0.5 ppm were added. Color changes were observed, and absorbance was measured using a UV-Vis spectrophotometer, with RGB values measured by the TCS3200 color sensor as the proposed method.

Validation method

Method validation was conducted using 5 parameters: Accuracy, precision, linearity, detection limit (DL), and limit of quantification (LoQ).

Statistical analysis

Statistically analysis was performed to compared the results obtained using the TCS3200 color sensor, as the proposed method, to those from the standard UV-Vis spectrophotometer method. The comparison was conducted using a 2-tailed t-test, where the calculated t-value ($t_{calculated}$) for each technique was compared to the critical t-value (t_{table}); if $t_{calculated} < t_{table}$, it can be concluded that the TCS3200 color sensor method provides equivalent results or statistically comparable to the UV-Vis spectrophotometer method for determination mercury ions levels in river water samples.

Results and discussion

Extraction of *Moringa* leaves

The percentage yields from the extraction of 203.886 g of *Moringa* leaves using ethanol and ethyl acetate as solvents are shown in **Table 1**. The ethanol extract yielded 48.77 g with a percentage yield of 23.92 %, whereas the ethyl acetate extract from the partitioning process yielded 6.98 g with a percentage yield of 14.32 %.

Table 1 Yield obtained of *Moringa* leaf extract from maceration process.

Sample	Weight (g)	Percentage Yield (%)
MOE1	48.77	23.92
MOEA	6.98	14.32
Residue	148.14	61.70

MOE1: Ethanol extract of *Moringa* leaves; MOEA: Ethyl acetate extract of *Moringa* leaves.

Qualitative tests for phenolics and flavonoids content

The qualitative tests for phenolics and flavonoids serve as an initial screening to confirm the presence of these compounds in *Moringa* leaves, which can act as bio-reductors in the synthesis of AgNPs. As indicated in **Table 2**, the *Moringa* leaf extract tested positive for phenolics and flavonoids content.

Table 2 Qualitative test for phenolics and flavonoids in *Moringa* leaves extract.

Sample	Phytochemical test	Color	Result
Ethanol Extract	Phenolics	Dark Green	+
	Flavonoids	Brick Red	+
Ethyl Acetate Extract	Phenolics	Blackish Green	+
	Flavonoids	Reddish Purple	+

+ means that the testing is positive results.

Quantitative tests for phenolics and flavonoids

TPC testing

The TPC in the *Moringa* leaf extract was determined using the Folin-Ciocalteu method, with gallic acid as the standard. Absorbance values from varying concentrations of gallic acid were used to construct a calibration curve. The total phenolic content of the *Moringa* leaf extract was calculated using the regression equation derived from the calibration curve $y = 0.0008x - 0.0224$, with $R^2 = 0.997$ as shown in **Figure 2**.

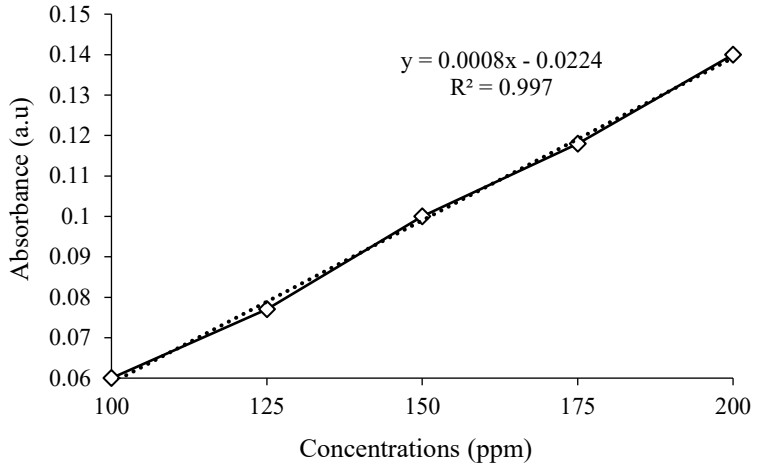

Figure 2 Gallic acid calibration curve.

The highest total phenolic content was found in the ethanol extract of *Moringa* leaves, with a value of 133 mg GAE/g, while the ethyl acetate extract contained a total phenolic content of 54.25 mg GAE/g, as shown in **Table 3**.

Table 3 TPC measurement.

Sample	Absorbance ($\bar{x}$)	TPC (mg GAE/g)
MOE1	0.084	133.000
MOEA	0.021	54.250

TPC: Total phenolic content; MOE1: Ethanol extract of *Moringa* leaves; MOEA: Ethyl acetate extract of *Moringa* leaves.

TFC testing

The total flavonoid content was determined using $AlCl_3$ and quercetin (QE) as the standard solution. Absorbance values from different concentrations of the quercetin standard solution were used to create a calibration curve. Based on **Figure 3**, the regression equation from the quercetin calibration curve, y = 0.0069x + 0.0249 (R^2 = 0.9847) was used to determine the total flavonoid content in the *Moringa* leaf extract by substituting the extract's absorbance values into the regression equation.

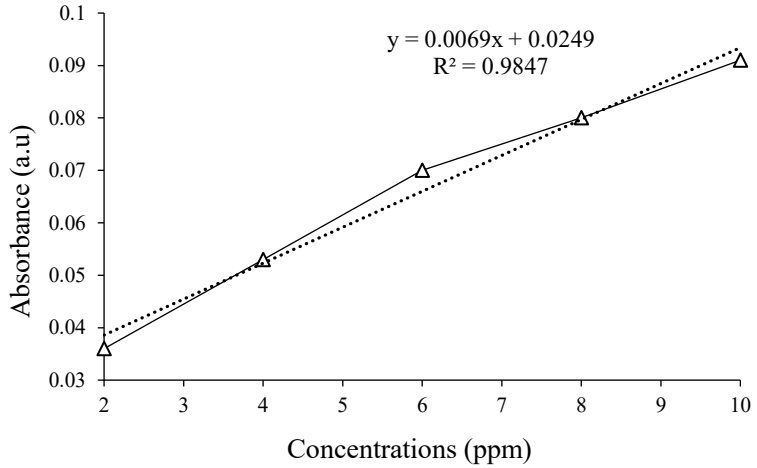

Figure 3 Quercetin calibration curve.

The ethyl acetate extract of Moringa leaves was selected due to its significantly TFC (11.319 mg QE/g) compared to the ethanol extract (1.754 mg QE/g) (**Table 4**). TFC in this study is higher than early reported study from *Lantana camara* extract [50]. Flavonoids are known for their strong affinity for metal ions and their dual role as reducing and stabilizing agents during nanoparticle synthesis [51]. During the biosynthesis of AgNPs, flavonoids facilitate the reduction of Ag^+ ions to Ag^0 by donating electrons while simultaneously stabilizing the nanoparticles to prevent aggregation [52,53]. The high flavonoid concentration in the ethyl acetate extract enhances its effectiveness in this process, making it a best choice for AgNP synthesis by improving both efficiency and stability.

Table 4 TFC measurement.

Sample	Absorbance ($\bar{x}$)	TFC (mg QE/g)
MOE1	0.037	1.754
MOEA	0.103	11.319

MOE1: Ethanol extract of *Moringa* leaves, MOEA: Ethyl acetate extract of *Moringa* leaves.

Synthesis of AgNPs

The color change of the solution from pale yellow to yellowish-brown after adding $AgNO_3$ and heating serves as an initial indicator of AgNPs formation. This change signifies the reduction of $AgNO_3$ (Ag^+) to Ag^0 in the form of AgNPs [54] as shown in **Figure 4**. Study have shown that *Moringa oleifera* extract have used as stabilizer and reducing the metallic NPs [55]. This finding is align with previous reported study, synthesis of AgNPs using *Sideritis montana* L. leaf extract [56] and from synthesized using walnut leaves according to a straightforward method [57]. Similarly, Dubay *et al*. [58], reported tha, the color change observed during the synthesis of AgNPs using *Eucalyptus hybrida* leaf extract is due to the presence of terpenoids and flavonoids in the leaf extract, which are likely active compounds stabilizing the AgNPs. The color change is attributed to surface plasmon resonance (SPR), resulting from the excitation of electrons on the surface of the AgNPs [22,47].

(A) (B) (C)

Figure 4 Solution of: At the start of heating (A); after heating (B); after 1 day incubation (C) during AgNPs synthesis.

The synthesized AgNPs were analyzed to determine the maximum wavelength (λ_{max}) using a UV-Vis spectrophotometer in the 380 - 500 nm range. The measurements showed that the AgNPs exhibited a λ_{max} at 410 nm peak absorbance of 0.750 as shown in the **Figure 5**. These results align with theoretical expectations, as AgNPs typically have a maximum wavelength ranging from 400 - 450 nm [59,60].

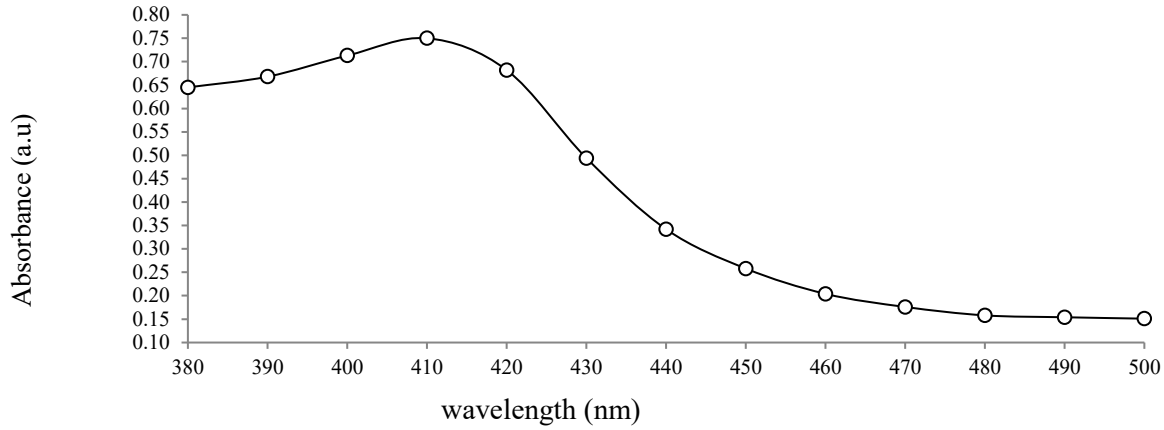

Figure 5 AgNPs λ_{max} measurement curve.

Characterization of AgNPs

FTIR

Silver nanoparticles (AgNPs) were characterized using fourier transform infrared spectroscopy. FTIR characterization was performed to identify potential interactions between $AgNO_3$ and active compounds in the extract that may act as bio-reductors during nanoparticle synthesis [47]. The FTIR characterization results are shown in **Figure 6**. The FTIR spectrum of the ethanol extract of *Moringa* leaves exhibits a broad and strong absorption band at 3,375 cm^{-1}, which is characteristic of hydroxyl (-OH) groups in alcohol and phenolic compounds. Additionally, a sharp absorption band at 1,641 cm^{-1} indicates the presence of carbonyl (C=O) groups in the ethyl acetate extract of *Moringa* leaves, while the band at 681 cm^{-1} suggests the presence of alkene (C-H) groups (**Figure 6(a)**). **Figure 6(b)** presents the FTIR spectrum of AgNPs synthesized using the ethyl acetate extract of *Moringa* leaves as a bio-reductor. This spectrum shows the disappearance of the peak at 681 cm^{-1}, along with a shift in the wavenumbers of the -OH and C=O groups to 3,356 and 1,636 cm^{-1}, respectively. The shift in the -OH group wavenumber indicates an interaction between the -OH group and Ag due to the redox process [25]. The presence of -OH groups in the *Moringa* leaf extract suggests the involvement of polyphenol or flavonoid compounds as bio-reductors and stabilizers in the synthesis of AgNPs [29,47].

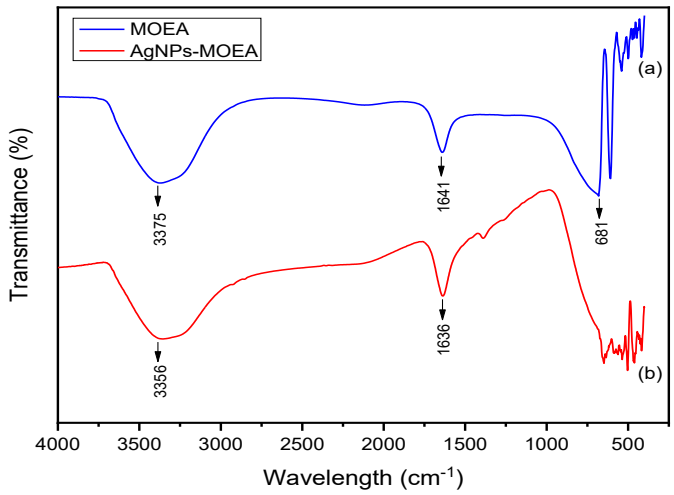

Figure 6 FTIR spectrum of (a) MOEA Extract; (b) AgNPs. MOEA: Ethyl acetate extract of *Moringa* leaves; AgNPs: Silver nanoparticles.

TEM

AgNPs were characterized using TEM to determine the particle size distribution and morphological shape of the synthesized AgNPs [31,47]. TEM characterization is depicted in **Figure 7**. Particle size distribution of AgNPs was measured using TEM

images, supported by ImageJ and OriginPro software, to determine the size distribution of AgNPs synthesized using *Moringa oleifera* leaf extract. **Figure 9** show that the AgNPs synthesized from the ethyl acetate extract of *Moringa* leaves (MOEA) exhibit a spherical morphology, with a diverse particle size distribution ranging from 5 to 35 nm. The AgNPs are predominantly sized between 15 and 20 nm, with an average particle size of 17.233 nm.

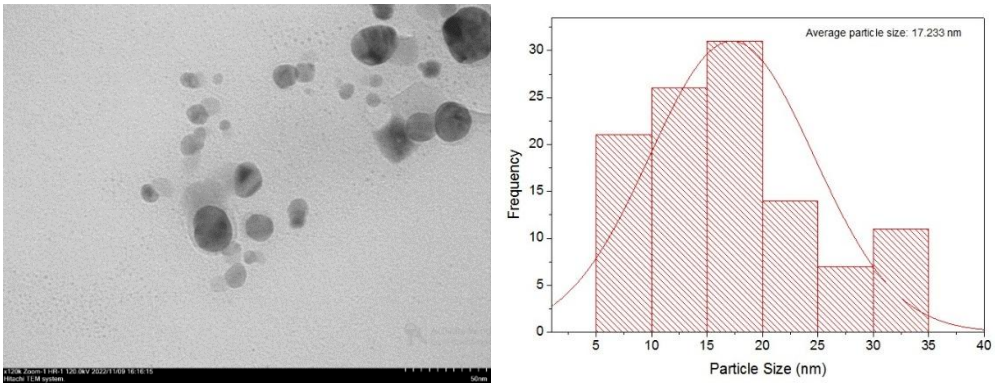

(A) (B)

Figure 7 TEM characterization (A); and particle size distribution (B) of AgNPs MOEA.

Detection of Hg^{2+} metal ions

Calibration curve preparation

The calibration curve is prepared to determine the mercury ions concentration in samples. Measurements were conducted using UV-Vis spectrophotometry and the TCS3200 color sensor as the proposed method. According to **Figure 8**, the UV-Vis spectrophotometer calibration curve shows that the absorbance value decreases as the concentration of Hg^{2+} added to the AgNPs increases. This occurs due to the oxidation process of Ag^0 in the AgNPs, which intensifies with increasing Hg^{2+} concentration. The resulting regression equation $y = –0.1x + 0.4644$ with a coefficient of determination (R^2) of 0.9968.

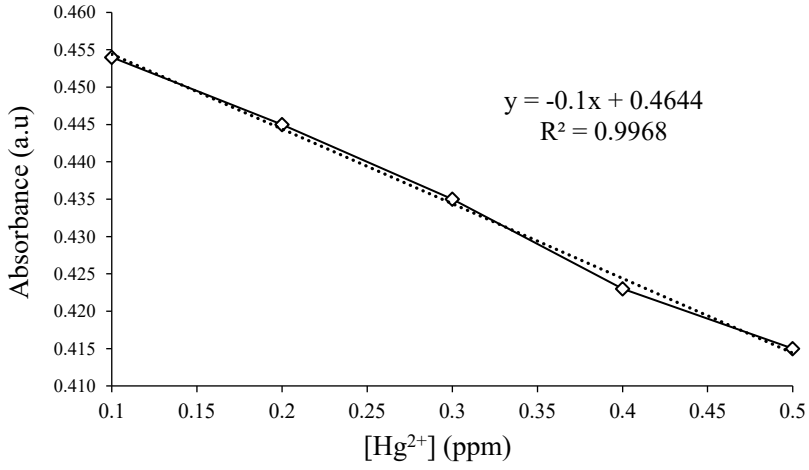

Figure 8 UV-Vis Spectrophotometer calibration curve.

Figure 9 shows the calibration curve using the color sensor. The TCS3200 color sensor calibration resulted in 3 regression equations for each RGB index value. In this study, the blue (IB) index was chosen because it has the best slope, even though its R^2 value is slightly lower. The regression equation for IB is $y = 0.164x + 0.221$, with an R^2 value of 0.9849, which is still sufficiently high. Therefore, the IB regression equation was used to determine the mercury ion levels in the samples.

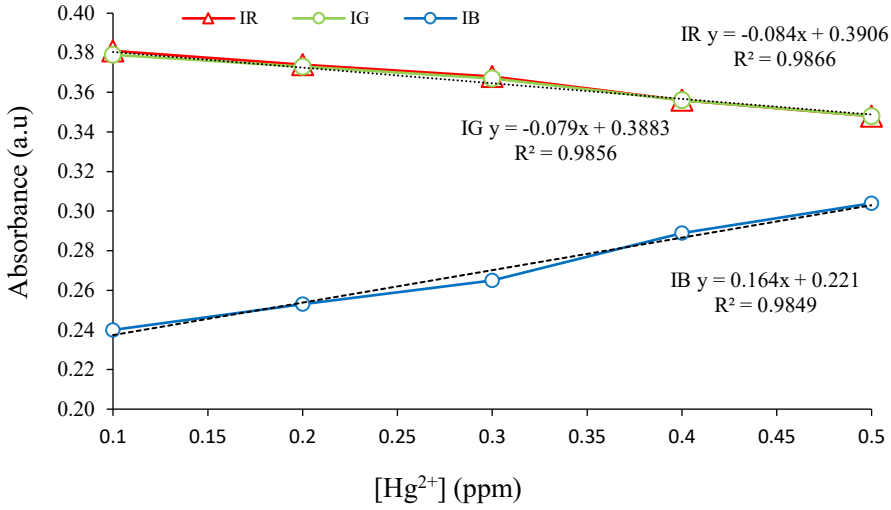

Figure 9 TCS3200 color sensor calibration curve. IR, IG and IB: Index color of red, green and blue, respectively.

Determination of Hg^{2+} metal ions concentration

The mercury ions concentration results are shown in **Table 5**. According to **Table 5**, Sample C exhibits the lowest absorbance and the highest mercury ions concentration among the samples at 0.284 ppm. The low absorbance indicates the oxidation of AgNPs by mercury ions present in the sample. Consequently, an increase in mercury ions in the sample leads to enhanced oxidation, resulting in decreased absorbance of the AgNPs solution with the sample. Similarly, **Table 5** also shown consistent results using the color sensor method, with Sample C having the highest mercury ions concentration at 0.287 ppm. The mercury ions concentration in the sample is calculated by substituting the IB value from the sample into the IB regression equation from the calibration curve.

Table 5 Mercury ions level in samples using UV-Vis spectrophotometer and TCS3200 color sensor.

Samples	UV-Vis		Color sensor	
	Absorbance (x̄)	Concentration (ppm)	Average I_R	Concentration (ppm)
A	0.444	0.204	0.256	0.213
B	0.451	0.134	0.242	0.128
C	0.436	0.284	0.268	0.287

Sensitivity

Selectivity testing was conducted to determine which metal ions the AgNPs (AgNPs) are selective for. The results of the selectivity test are presented in **Figure 10**. According to **Figure 10(A)**, the most significant change in absorbance occurs with AgNPs treated with Hg^{2+} ions, where the absorbance decreases from 0.750 to 0.350 after adding Hg^{2+} ions. This indicates that mercury ions can oxidize Ag^0 in the AgNPs to Ag^+ ions. **Figure 10(B)** shows the selectivity measurements using the TCS3200 color sensor. AgNPs exposed to mercury ions exhibit the highest blue intensity value compared to other metals. Therefore, it can be concluded that the AgNPs synthesized from *Moringa* leaf extract are selective for Hg^{2+} ions.

This sensitivity is consistent with previous studies, which reported that the interaction between Hg^{2+} ions and AgNPs often triggers a redox reaction-where Hg^{2+} oxidizes Ag^0 to Ag^+-leading to a decrease in absorbance and a visible color change from yellow to colorless [61,62]. Additionally, the localized LSPR band of AgNPs is known to shift in the presence of Hg^{2+}, a commonly used indicator of selectivity in optical sensors [63]. Similar behavior has also been observed in AgNPs synthesized using other plant-based and biopolymer methods, such as Equisetum diffusum and silk sericin, which showed high sensitivity to Hg^{2+}

through distinct optical changes [20,61]. The sensitivity levels in previous reports vary depending on the synthesis method and surface functionality, with reported detection limits ranging from 15 ppb to 1 ppm [61,64]. Therefore, the synthesized AgNPs in this study demonstrate comparable or potentially improved selectivity for mercury ions.

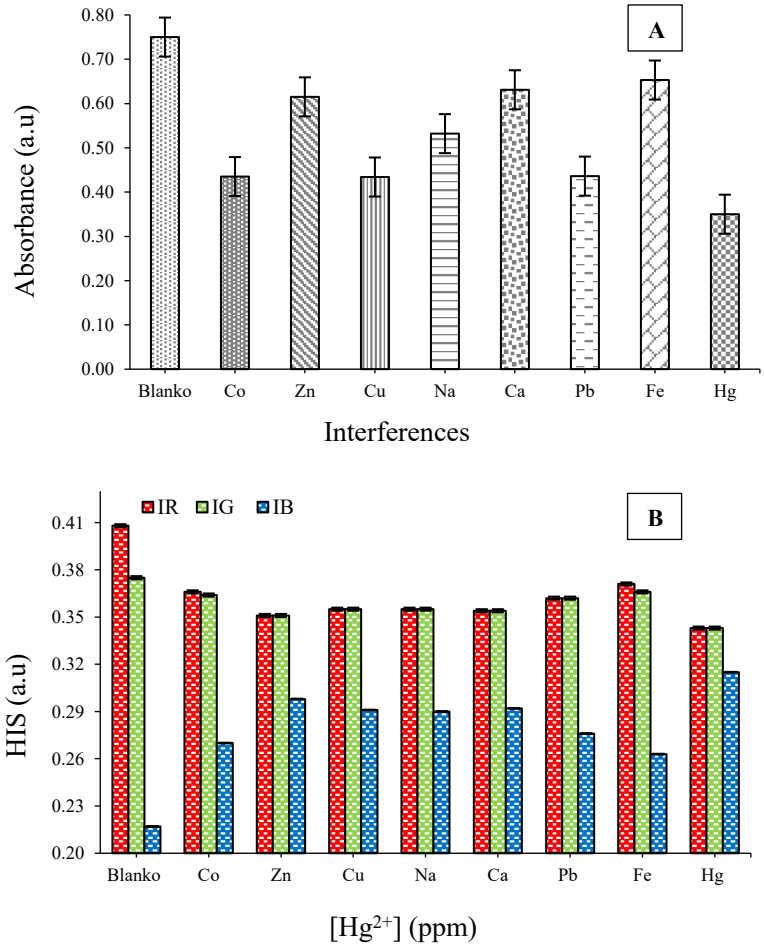

Figure 10 Selectivity testing using: UV-Vis Spectrophotometer (A); TCS3200 color sensor (B).

Specificity testing

Specificity testing was conducted to ensure that the AgNPs react positively only to mercury ions, indicated by a color change from yellow to clear, and not to other metal ions that may be present in the sample. The color change from yellow to clear occurs due to the redox process between mercury ions and AgNPs, where Ag^0 in the nanoparticles is oxidized by Hg^{2+} ions [22]. The results of the specificity test can be seen in **Figure 11** and **Table 6**.

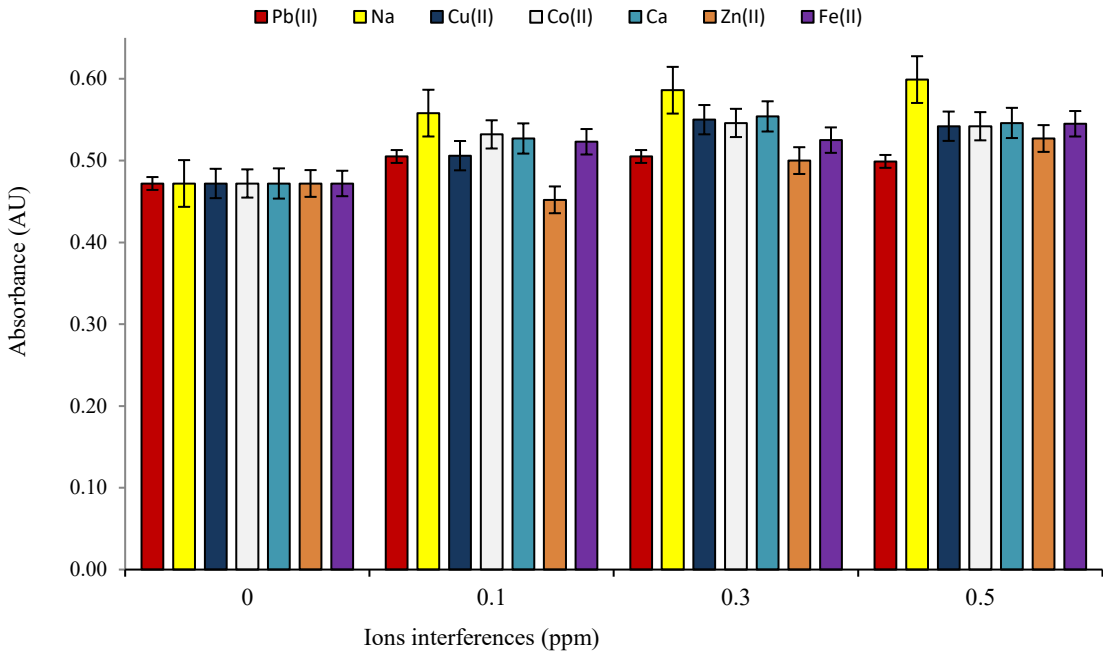

Figure 11 Specificity Testing with UV-Vis Spectrophotometer.

Table 6 HIS Values from specificity testing with TCS3200 color sensor.

Sample	HIS			Color	Color scale		
	IR	IG	IB		Red	Green	Blue
AgNPs	0.372	0.363	0.265		226	208	120
AgNPs + Hg (Positive control)	0.343	0.343	0.315		255	255	234
---- → Pb 0.1 ppm	0.343	0.346	0.311		249	251	226
---- → Pb 0.3 ppm	0.346	0.347	0.307		244	245	217
---- → Pb 0.5 ppm	0.346	0.344	0.310		243	242	218
AgNPs + Hg + Zn 0.1 ppm	0.343	0.340	0.317		241	239	223
---- → Zn 0.3 ppm	0.348	0.344	0.308		239	236	211
---- → Zn 0.5 ppm	0.341	0.341	0.318		245	245	229
AgNPs + Hg + Co 0.1 ppm	0.350	0.350	0.299		255	255	218
---- → Co 0.3 ppm	0.352	0.352	0.297		255	255	215
---- → Co 0.5 ppm	0.353	0.352	0.295		255	254	213
AgNPs + Hg + Na 0.1 ppm	0.361	0.354	0.286		254	249	201
---- → Na 0.3 ppm	0.361	0.354	0.286		255	250	202
---- → Na 0.5 ppm	0.363	0.354	0.283		255	249	199
AgNPs + Hg + Ca 0.1 ppm	0.350	0.350	0.299		255	255	218
---- → Ca 0.3 ppm	0.352	0.350	0.298		255	254	216
---- → Ca 0.5 ppm	0.352	0.352	0.297		255	255	215
AgNPs + Hg + Cu 0.1 ppm	0.348	0.348	0.304		255	255	223

Sample	HIS			Color	Color scale		
	IR	IG	IB		Red	Green	Blue
---- → Cu 0.3 ppm	0.350	0.350	0.300		255	255	219
---- → Cu 0.5 ppm	0.353	0.352	0.295		255	254	213
AgNPs + Hg + Fe 0.1 ppm	0.340	0.340	0.319		255	255	239
---- → Fe 0.3 ppm	0.349	0.349	0.302		255	255	221
---- → Fe 0.5 ppm	0.350	0.350	0.299		255	255	218

HIS, IR, IG, IB was hue – intensity – saturation, index of red, green, and blue, respectively.

According to Table 6, the AgNPs treated with mercury ions showed a color change to clear, indicating specificity to mercury ions. In contrast, the silver nanoparticle solutions treated with mercury ions and other metal mixtures showed no significant color change. However, the Intensity Blue (IB) value increased for each NPP solution after adding mercury ions and other metals, suggesting that the solution color faded. This indicates the oxidation of AgNPs by mercury ions. Therefore, it can be concluded that the NPP synthesized from *Moringa* leaf extract is specific to mercury ions when measured using the TCS3200 color sensor. The specificity test results using the UV-Vis spectrophotometer are shown in **Figure 13**. According to **Figure 14**, an increase in absorbance values of silver nanoparticle solutions was observed after adding foreign metal ions. However, this increase in absorbance was not significant enough to indicate a lack of specificity, suggesting that the AgNPs synthesized from *Moringa* leaf extract remain specific to mercury ions, albeit with low specificity when measured using the UV-Vis spectrophotometer.

Sensitivity testing

The sensitivity testing results are shown in **Figure 12**. Result in **Figure 12(A)** demonstrates that as more Hg^{2+} ions are added to the AgNPs, the absorbance values decrease. In contrast, in the measurements with the TCS3200 color sensor, shown in **Figure 12(B)**, the blue intensity values increase with the addition of Hg^{2+} ions, indicating that the solution's color becomes more faded. This occurs due to the increasing oxidation process of Ag^0 in the nanoparticles as Hg^{2+} concentration increases.

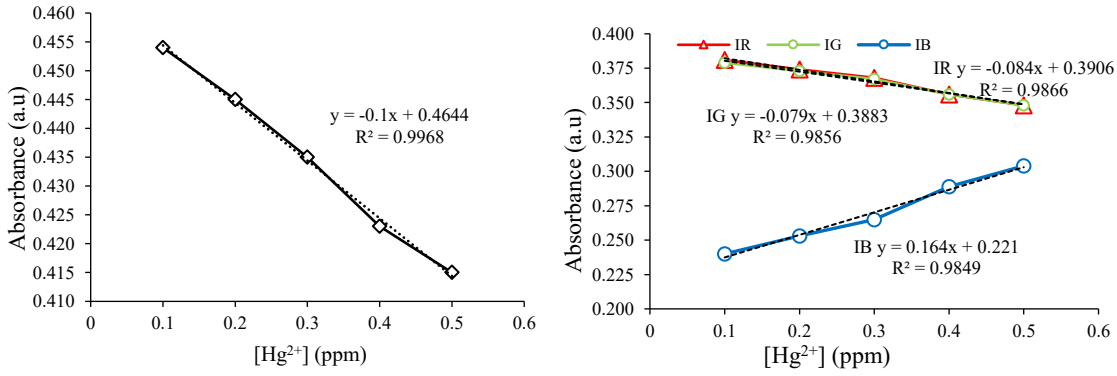

(A) (B)

Figure 12 Sensitivity testing using (a) UV-Vis spectrophotometer and (b) TCS3200 color sensor. IR, IG and IB: Index color of red, green and blue, respectively.

Based on **Figure 12**, the sensitivity value for the UV-Vis spectrophotometer is 0.01, derived from the regression equation y = –0.01x + 0.4644, with an R^2 value of 0.9968. In the TCS3200 color sensor measurements, a sensitivity value of 0.164 is obtained

from the regression equation y = 0.164x + 0.3906 with an R^2 value of 0.9849.

Validation method

Accuracy and precisions

The method's accuracy is expressed as the percentage recovery (% recovery), which reflects the closeness of the measured concentration to the true concentration of the standard solution [65-67]. The % recovery values for both methods are presented in **Table 7**. The UV-Vis spectrophotometer method showed a % recovery range of 98 - 104 %, while the color sensor method exhibited a % recovery range of 89.3 - 110 %. These results align with theoretical expectations, as Dhanshri [68], suggests that acceptable accuracy is achieved when the % recovery falls within the range of 70 - 130 %.

Table 7 Percentage recovery (% recovery) (n = 3) and RSD values for both methods.

Concentration (ppm)	True Concentration		% Recovery		% RSD	
	Color sensor	UV-Vis	Color sensor	UV-Vis	Color sensor	UV-Vis
0.1	0.110	0.104	110.0	104.0	1.255	0.220
0.3	0.268	0.294	89.3	98.0	0.755	0.230
0.5	0.512	0.494	102.4	98.8	0.328	0.241

Precision measures the degree of repeatability of an analytical method, providing consistent results across multiple repetitions [67]. The precision test analyzed 3 concentrations with 3 repetitions for each concentration. The measurement methods used were the UV-Vis spectrophotometer as a reference and the TCS3200 Color Sensor as the proposed method. Precision is expressed in terms of % RSD (relative standard deviation). The % RSD values for both measurement methods are shown in **Table 7**. According to Patil *et al.* [69], a method is considered to have good precision if % RSD < 3 %. As shown in Table 8, both testing methods exhibit good precision with % RSD values of less than 3 %.

In this study, precision testing was also performed both intraday and interday, which measures precision under the same conditions but with different durations. For intraday precision, measurements were taken on the same day at different durations: 0, 30, 60, and 90 min. For interday precision, measurements were taken on different days with the same duration: 0, 1, 2 and 3 days. The intraday and interday precision test results are expressed in % RSD and shown in **Table 8**. Based on **Table 8**, the intraday and interday precision tests for both methods resulted in % RSD < 1 %. This indicates that both the UV-Vis spectrophotometer and the TCS3200 Color Sensor, as the proposed method, fall into the category of highly precise measurements.

Table 8 % RSD values for intraday and interday precision.

Duration (min)	Intraday precision		Interday precision	
	% RSD			
	UV-Vis	Color sensor	UV-Vis	Color sensor
0	0.258	0.297	0.258	0.297
30	0.233	0.295	0.212	0.289
60	0.228	0.294	0.482	0.295
90	0.220	0.292	0.483	0.296

Linearity

According to Swetha and Pooja [70], linearity reflects the ability of a measuring instrument to produce results that are directly proportional to the concentration of the analyte in a sample. Linearity demonstrates how well the standard curve connects absorbance (y) with concentration (x). The linearity test results can be seen based on the standard curves of the UV-Vis

spectrophotometer and the TCS3200 color sensor shown in **Figures 11** and **12**. It is evident that the concentration range of 0.1 - 0.5 ppm is linear for the color sensor with a correlation coefficient of 0.9849 and for the UV-Vis spectrophotometer with a correlation coefficient of 0.9968. A correlation coefficient close to 1 indicates that the UV-Vis spectrophotometer and the TCS3200 color sensor exhibit good linearity as recommended methods [71,72].

DL and LoQ

The DL is the smallest amount of analyte in a sample that can be detected while still providing a significant response compared to the blank. In contrast, the LoQ is the smallest amount of analyte that can be quantitatively determined with acceptable precision and accuracy. The DL and LoQ values for both measurement methods are shown in **Table 9**, indicating that the DL or lowest concentration of Hg^{2+} detectable by both the UV-Vis spectrophotometer and the TCS3200 color sensor are 0.03 and 0.069 ppm, respectively. The LoQ or lowest concentration of Hg^{2+} that can be determined with acceptable precision and accuracy for both methods is 0.1 ppm for the UV-Vis spectrophotometer and 0.230 ppm for the TCS3200 color sensor.

Table 9 DL and LoQ values for both methods.

Validation method	UV-Vis (ppm)	Color sensor (ppm)
DL	0.030	0.069
LoQ	0.100	0.230

Statistical analysis

The method comparison was conducted to determine if the results obtained using the TCS3200 Color Sensor are consistent with those obtained using the UV-Vis spectrophotometry method. In this study, a 2-tailed t-test was employed for the method comparison. The 2-tailed t-test involved calculating the $t_{calculated}$ value for each method and comparing it with the t_{table} value. If $t_{calculated} < t_{table}$, it can be concluded that the TCS3200 Color Sensor method yields result equivalent to those of the UV-Vis spectrophotometer for measuring mercury ions levels in river water samples. The comparative measurement results of the 2 methods are presented in **Table 10**.

Table 10 Two-tailed t-test calculation on samples with both testing methods.

Descriptions	TCS3200 color sensor			UV-Vis		
	x (ppm)	$x-\bar{x}$	$(x-\bar{x})^2$	x (ppm)	$x-\bar{x}$	$(x-\bar{x})^2$
Sample A	0.213	0.004	0.000016	0.204	–0.003	0.000009
Sample B	0.128	–0.081	0.006561	0.134	–0.073	0.005329
Sample C	0.287	0.078	0.006084	0.284	0.077	0.005929
Total	0.628		0.012661	0.622		0.011267
Average	0.209			0.207		
Total data (n)		3			3	
Standard deviation (STD)		0.080			0.075	
S^2		0.0063			0.0056	
t-calculated			0.032			
t-table			2.776			

Table 10 shows that the highest concentration of Hg, as measured by both the UV-Vis spectrophotometer and the TCS3200 Color Sensor, was found in sample C. Furthermore, the measurement results of mercury ions levels in the samples using both methods do not show any significant differences. However, a 2-tailed t-test

was conducted to ensure valid results with a 95 % confidence interval and 4 degrees of freedom (df). The test yielded a $t_{calculated}$ value of 0.032 and a t_{table} value of 2.776. Thus, since $t_{calculated} < t_{table}$, it can be concluded that the measurement method using the TCS3200 Color Sensor is as effective as the UV-Vis spectrophotometer method. This comparison confirms the reliability and accuracy of the TCS3200 Color Sensor for measuring mercury ions concentrations in environmental samples, offering a comparable alternative to the traditional UV-Vis spectrophotometry method

Conclusions

Moringa oleifera leaf extract can be used as a reducing agent in the biosynthesis of AgNPs, which are selective and specific to Hg metal. The Arduino Uno-based TCS3200 Color Sensor can detect mercury ions using AgNPs synthesized with *Moringa* leaf ethyl acetate extract, achieving an accuracy (% recovery) range of 89.3 - 110 % and a DL as low as 0.069 ppm. A 2-tailed t-test comparison of methods confirmed that the TCS3200 Color Sensor is as effective as the UV-Vis spectrophotometer. The highest mercury ions concentration in river water samples detected by the TCS3200 Color Sensor was found in sample C at 0.287 ppm. This method offers a low cost, sustainability, and real-time for resource-limited areas.

References

[1] S Song, Y Li, QS Liu, H Wang, P Li, J Shi, L Hu, H Zhang, Y Liu, K Li, X Zhao and Z Cai. Interaction of mercury ion (Hg^{2+}) with blood and cytotoxicity attenuation by serum albumin binding. *Journal of Hazardous Materials* 2021; **412**, 125158.

[2] PB Tchounwou, CG Yedjou, AK Patlolla and DJ Sutton. *Heavy metal toxicity and the environment*. *In*: A Luch (Ed.). Molecular, clinical and environmental toxicology. Springer Basel, Basel, Switzerland, 2012.

[3] S Singh, A Numan, Y Zhan, V Singh, TV Hung and ND Nam. A novel highly efficient and ultrasensitive electrochemical detection of toxic mercury (II) ions in canned tuna fish and tap water based on a copper metal-organic framework. *Journal of Hazardous Materials* 2020; **399**, 123042.

[4] Y Wang, L Zhang, X Han, L Zhang, X Wang and L Chen. Fluorescent probe for mercury ion imaging analysis: Strategies and applications. *Chemical Engineering Journal* 2021; **406**, 127166.

[5] F Huisa-Mamani, A Arizaca-Avalos and OE Llanque-Maquera. Mercury pollution in water, soil, and biota induced by artisanal gold mining: A case study from Ananea District, Puno, Peru. *Journal of Degraded and Mining Lands Management* 2025; **12(2)**, 7159-7171.

[6] P Prema, V Veeramanikandan, K Rameshkumar, MK Gatasheh, AA Hatamleh, R Balasubramani and P Balaji. Statistical optimization of silver nanoparticle synthesis by green tea extract and its efficacy on colorimetric detection of mercury from industrial wastewater. *Environmental Research* 2022; **204**, 111915.

[7] S Balasurya, A Syed, AM Thomas, N Marraiki, S Al-Rashed, AM Elgorban, LL Raju, A Das and SS Khan. Colorimetric detection of mercury ions from environmental water sample by using 3-(Trimethoxysilyl)propyl methacrylate functionalized Ag NPs-tryptophan nanoconjugate. *Journal of Photochemistry and Photobiology B: Biology* 2020; **207**, 111888.

[8] D King, M Watts, E Hamilton, R Mortimer, M Coffey, O Osano and MD Bonito. Mercury speciation in environmental samples associated with artisanal small-scale gold mines using a novel solid-phase extraction approach to sample collection and preservation. *Environmental Geochemistry and Health* 2024; **46(11)**, 481.

[9] J Słowik and H Ćwirko. The impact of mercury on human health. *Medical Science Pulse* 2024; **18(4)**, 39-52.

[10] AA Lysenko. Hygienic and biochemical aspects of the effect of mercury on the human body (literature review). *Hygiene and Sanitation* 2024; **103(11)**, 1447-1451.

[11] FH Narouei, L Livernois, D Andreescu and S Andreescu. Highly sensitive mercury detection using electroactive gold-decorated polymer nanofibers. *Sensors and Actuators B: Chemical* 2021; **329**, 129267.

[12] World Health Organization. *Mercury and human health: Educational course*. World Health Organization, Geneva, Switzerland, 2021.

[13] E Mohammed, T Mohammed and A Mohammed. Optimization of instrument conditions for the analysis of mercury, arsenic, antimony and selenium by atomic absorption spectroscopy. *MethodsX* 2018; **5**, 824-833.

[14] Z Wittmann. Determination of mercury by atomic-absorption spectrophotometry. *Talanta* 1981; **28(4)**, 271-273.

[15] HI Qudus, P Purwadi, I Holilah and S Hadi. Analysis of mercury in skin lightening cream by microwave plasma atomic emission spectroscopy (MP-AES). *Molecules* 2021; **26(11)**, 3130.

[16] V Balaram. Microwave plasma atomic emission spectrometry (MP-AES) and its applications - a critical review. *Microchemical Journal* 2020; **159(1997)**, 105483.

[17] B Passariello, M Barbaro, S Quaresima, A Casciello and A Marabini. Determination of mercury by inductively coupled plasma-mass spectrometry. *Microchemical Journal* 1996; **54(4)**, 348-354.

[18] SC Wilschefski and MR Baxter. Inductively coupled plasma mass spectrometry: Introduction to analytical aspects. *Clinical Biochemistry Reviews* 2019; **40(3)**, 115-133.

[19] M Winter, F Lessmann and V Harth. A method for reliable quantification of mercury in occupational and environmental medical urine samples by inductively coupled plasma mass spectrometry. *Analytical Methods* 2023; **15(16)**, 2030-2038.

[20] A Jabbar, A Abbas, N Assad, M Naeem-Ul-Hassan, HA Alhazmi, A Najmi, K Zoghebi, MA Bratty, A Hanbashi and HMA Amin. A highly selective Hg^{2+} colorimetric sensor and antimicrobial agent based on green synthesized silver nanoparticles using Equisetum diffusum extract. *RSC Advances* 2023; **13(41)**, 28666-28675.

[21] E Alzahrani. Colorimetric detection based on localized surface plasmon resonance optical characteristics for sensing of mercury using green-synthesized silver nanoparticles. *Journal of Analytical Methods in Chemistry* 2020; **2020(4)**, 1-14.

[22] D Demirezen Yılmaz, D Aksu Demirezen and H Mıhçıokur. Colorimetric detection of mercury ion using chlorophyll functionalized green silver nanoparticles in aqueous medium. *Surfaces and Interfaces* 2021; **22(25)**, 100840.

[23] R Kataria, K Sethuraman, D Vashisht, A Vashisht, SK Mehta and A Gupta. Colorimetric detection of mercury ions based on anti-aggregation of gold nanoparticles using 3,5-dimethyl-1-thiocarboxamidepyrazole. *Microchemical Journal* 2019; **148**, 299-305.

[24] P Saha, MM Billah, ABMN Islam, MA Habib and M Mahiuddin. Green synthesized silver nanoparticles: A potential antibacterial agent, antioxidant, and colorimetric nanoprobe for the detection of Hg^{2+} ions. *Global Challenges* 2023; **7(8)**, e202300072.

[25] M Ismail, W Xiangke, AA Khan and Q Khan. Amomum subalatum leaf extract-derived silver nanoparticles for eco-friendly spectrophotometric detection of Hg^{2+} ions in water. *Chemical Physics Impact* 2023; **6**, 100148.

[26] C Pechyen, B Tangnorawich, S Toommee, R Marks and Y Parcharoen. Green synthesis of metal nanoparticles, characterization, and biosensing applications. *Sensors International* 2024; **5(4)**, 100287.

[27] R Memon, AA Memon, Siraj Uddin, A Balouch, K Memon, STH Sherazi, AA Chandio and R Kumar. Ultrasensitive colorimetric detection of Hg^{2+} in aqueous media via green synthesis by Ziziphus mauritiana leaf extract-based silver nanoparticles. *International Journal of Environmental Analytical Chemistry* 2022; **102(18)**, 7046-7061.

[28] HM Mehwish, MSR Rajoka, Y Xiong, H Cai, RM Aadil, Q Mahmood, Z He and Q Zhu. Green synthesis of a silver nanoparticle using Moringa oleifera seed and its applications for antimicrobial and sun-light mediated photocatalytic water detoxification. *Journal of Environmental Chemical Engineering* 2021; **9(4)**, 105290.

[29] ABA Mohammed, A Mohamed, NEA El-Naggar, H Mahrous, GM Nasr, A Abdella, RH Ahmed, S Irmak, MSA Elsayed, S Selim, A Elkelish, DHM Alkhalifah, WN Hozzein and AS Ali. Antioxidant and antibacterial activities of silver nanoparticles biosynthesized by *Moringa oleifera* through response surface methodology. *Journal of Nanomaterials* 2022; **2022**, 9984308.

[30] K Suganandam, A Jeevalatha, C Kandeepan, N Kavitha, N Senthilkumar, S Sutha, MA Seyed, S Gandhi, S Ramya, GGL Pushpalatha, GC Abraham and R Jayakumararaj. Profile of phytochemicals and GC-MS analysis of bioactive compounds in natural dried-seed removed ripened pods methanolic extracts of Moringa oleifera. *Journal of Drug Delivery and Therapeutics* 2022; **12(5-S)**, 133-141.

[31] MR Bindhu, M Umadevi, GA Esmail, NA Al-Dhabi and MV Arasu. Green synthesis and characterization of silver nanoparticles from Moringa oleifera flower and assessment of antimicrobial and sensing properties. *Journal of Photochemistry and Photobiology B: Biology* 2020; **205**, 111836.

[32] A Pareek, M Pant, MM Gupta, P Kashania, Y Ratan, V Jain, A Pareek and AA Chuturgoon. Moringa oleifera: An updated comprehensive review of its pharmacological activities, ethnomedicinal, phytopharmaceutical formulation, clinical, phytochemical, and toxicological aspects. *International Journal of Molecular Sciences* 2023; **24(3)**, 2098.

[33] B Padayachee and H Baijnath. An updated comprehensive review of the medicinal, phytochemical and pharmacological properties of *Moringa oleifer*a. *South African Journal of Botany* 2020; **129**, 304-316.

[34] H Alkan, İH Ciğerci, MM Ali, O Hazman, R Liman, F Colă and E Bonciu. Cytotoxic and genotoxic evaluation of biosynthesized silver nanoparticles using Moringa oleifera on MCF-7 and HUVEC cell lines. *Plants* 2022; **11(10)**, 1293.

[35] K Suhud, Z Ula, M Dayanti, MS Surbakti, MD Hadistya, S Saleha, S Saiful, AA Kacaribu and MRF Damanik. Measurement of tartrazine levels in children's snacks in Banda Aceh using an Arduino Uno-based TCS3200 color sensor. *International Journal of Design & Nature and Ecodynamics* 2025; **20(1)**, 169-177.

[36] MS Surbakti, M Farhan, Z Zakaria, M Isa, E Sufriadi, S Alva, E Yusibani, L Heliawati, M Iqhrammullah and K Suhud. Development of Arduino Uno-based TCS3200 color sensor and its application on the determination of Rhodamine B level in syrup. *Indonesian Journal of Chemistry* 2022; **22(3)**, 630.

[37] K Suhud, S Sukoma, S Saleha and MS Surbakti. Development of TCS3200 color sensor based on Arduino Uno and its application in determining borax levels in food. *Indonesian Journal of Fundamental and Applied Chemistry* 2024, **9(2)**, 74-81.

[38] K Suhud, D Utari, MS Surbakti, S Alva, AF Omar, S Saiful, L Heliawati, P Ningsih, MD Hadistya, TZ Gunana, R Idroes and AA Kacaribu. Development of TCS3200 color sensor based on Arduino Uno microcontroller for determination of capsaicin level in sauces. *Sains Malaysiana* 2024; **53(12)**, 3339-3348.

[39] Z Fitri, M Adlim, MS Surbakti, AF Omar, FA Sijabat and S Syahreza. Mercury (II) ions assessment as a toxic waste hazard in solution based on imagery data for a part of environmental disaster management. *IOP Conference Series: Earth and Environmental Science* 2019; **273**, 012052.

[40] K Suhud, R Amalia, MS Surbakti, R Idroes, L Lelifajri, S Alva, H Ritonga, M Mazwan, MD Hadistya and AA Kacaribu. Arduino uno-based colorimetric sensor traction control system 3200 with AgNPs/PVP for Hg^{2+} detection in river water of Aceh Selatan Regency. *Indonesia, Journal of Ecological Engineering* 2025; **26(4)**, 45-58.

[41] M Dayanti, S Alva, Lelifajri, Nazaruddin, Julinawati, Sukoma, S Fonna, AK Arifin, SA Hasbullah, AA Kacaribu, M Said and K Suhud. Development of a mercury sensor using voltammetry techniques based on waste tire carbon electrodes modified with Zinc Oxide doped ion imprinted polypyrrole. *Sains Malaysiana* 2025; **54(4)**, 1063-1076.

[42] A Ogundipe, B Adetuyi, F Iheagwam, K Adefoyeke, J Olugbuyiro, O Ogunlana and O Ogunlana. *In vitro* experimental assessment of ethanolic extract of *Moringa oleifera* leaves as an α-amylase and α-lipase inhibitor. *Biochemistry Research International* 2022; **2022**, 4613109.

[43] G Bagheri, M Martorell, K Ramí¬rez-Alarcón, B Salehi and J Sharifi-Rad. Phytochemical screening of *Moringa oleifera* leaf extracts and their

antimicrobial activities. *Cellular and Molecular Biology* 2020; **66(1)**, 20-26.

[44] S Dubale, D Kebebe, A Zeynudin, N Abdissa and S Suleman. Phytochemical screening and antimicrobial activity evaluation of selected medicinal plants in Ethiopia. *Journal of Experimental Pharmacology* 2023; **15**, 51-62.

[45] I Maulana, B Ginting and K Azizah. Green synthesis of copper nanoparticles employing Annona squamosa L extract as antimicrobial and anticancer agents. *South African Journal of Chemical Engineering* 2023; **46(1)**, 65-71.

[46] R Yusnaini, R Nasution, N Saidi, T Arabia, R Idroes, I Ikhsan, R Bahtiar and M Iqhrammullah. Ethanolic extract from Limonia acidissima L. fruit attenuates serum uric acid level via URAT1 in potassium oxonate-induced hyperuricemic rats. *Pharmaceuticals* 2023; **16(3)**, 419.

[47] GM Mohammed and SN Hawar. Green biosynthesis of silver nanoparticles from *Moringa oleifera* leaves and its antimicrobial and cytotoxicity activities. *International Journal of Biomaterials* 2022; **2022**, 1-10.

[48] EA Shalaby, SMM Shanab, WMA El-Raheem and EA Hanafy. Biological activities and antioxidant potential of different biosynthesized nanoparticles of *Moringa oleifera*. *Scientific Reports* 2022; **12(1)**, 18400.

[49] M Valcárcel, A Gómez-Hens and S Rubio. Selectivity in analytical chemistry revisited. *Trends in Analytical Chemistry* 2001; **20(8)**, 386-393.

[50] P Kemala, R Idroes, K Khairan, M Ramli, B Ginting, Z Helwani, R Aulia, GM Idroes, Y Yusuf and R Efendi. Eco-friendly synthesis of silver nanoparticles: Enhancing optimization reaction, characterization, and antimicrobial properties with Lantana camara from geothermal area. *South African Journal of Chemical Engineering* 2025; **51(1)**, 57-67.

[51] DY Lestari, A Syoufian, PL Hariani, AJ Saviola, WC Oh, AK Amin, RA Pratika and K Wijaya. Facile green synthesis of silver nanoparticles decorated on sulfonated graphene oxide by rambutan (*Nephelium lappaceum*) leaf extract and application as a catalyst for converting benzene into nitrobenzene. *Results in Engineering* 2025; **25**, 104321.

[52] S Sysak, B Czarczynska-Goslinska, P Szyk, T Koczorowski, DT Mlynarczyk, W Szczolko, R Lesyk and T Goslinski. Metal nanoparticle-flavonoid connections: Synthesis, physicochemical and biological properties, as well as potential applications in medicine. *Nanomaterials* 2023; **13(9)**, 1531.

[53] T Hou, Y Guo, W Han, Y Zhou, VR Netala, H Li, H Li and Z Zhang. Exploring the biomedical applications of biosynthesized silver nanoparticles using Perilla frutescens flavonoid extract: Antibacterial, antioxidant, and cell toxicity properties against colon cancer cells. *Molecules* 2023; **28(17)**, 6431.

[54] N Genc, I Yildiz, R Chaoui, R Erenler, C Temiz and M Elmastas. Biosynthesis, characterization and antioxidant activity of oleuropein-mediated silver nanoparticles. *Inorganic and Nano-Metal Chemistry* 2021; **51(3)**, 411-419.

[55] PV Nagime, S Singh, VR Chidrawar, A Rajput, DM Syukri, NT Marwan and S Shafi. *Moringa oleifera*: A plethora of bioactive reservoirs with tremendous opportunity for green synthesis of silver nanoparticles enabled with multifaceted applications. *Nano-Structures & Nano-Objects* 2024; **40**, 101404.

[56] R Erenler and EN Gecer. Synthesis of silver nanoparticles using *Sideritis montana* L. leaf extract: Characterization, catalytic degradation of methylene blue and antioxidant activity. *Journal of Nano Research* 2022; **75**, 17-28.

[57] A Seçme, BM Bozer, A Yıldırım Kocaman, R Erenler and MH Calimli. Synthesis, characterization, and anticancer properties of Ag nanoparticles derived from walnut leaves tested on cells of L929, MCF-7 and H1299. *Journal of Drug Delivery Science and Technology* 2024; **94**, 105478.

[58] M Dubey, S Bhadauria and BS Kushwah. Green synthesis of nanosilver particles from extract of Eucalyptus hybrida (Safeda) leaf. *Digest Journal of Nanomaterials and Biostructures* 2009; **4(3)**, 537-543.

[59] JM Ashraf, MA Ansari, HM Khan, MA Alzohairy and I Choi. Green synthesis of silver nanoparticles

and characterization of their inhibitory effects on AGEs formation using biophysical techniques. *Scientific Reports* 2016; **6**, 20414.

[60] M Asif, R Yasmin, R Asif, A Ambreen, M Mustafa and S Umbreen. Green synthesis of silver nanoparticles (AgNPs), structural characterization, and their antibacterial potential. *Dose-Response* 2022; **20(2)**, 1-11.

[61] HK Sanjeevappa, P Nilogal, R Rayaraddy, LJ Martis, SM Osman, N Badiadka and S Yallappa. Biosynthesized unmodified silver nanoparticles: A colorimetric optical sensor for detection of Hg^{2+} ions in aqueous solution. *Results in Chemistry* 2022; **4(1-11)**, 100507.

[62] NM Abbasi, MU Hameed, N Nasim, F Ahmed, F Altaf, S Shahida, S Fayyaz, SM Sabir and P Bocchetta. Plasmonic nano silver: An efficient colorimetric sensor for the selective detection of Hg^{2+} ions in real samples. *Coatings* 2022; **12(6)**, 763.

[63] L Burratti, I Venditti, C Battocchio, S Casciardi and P Prosposito. Silver nanoparticles with different thiol functionalization: an opposite optical behaviour in presence of Hg(II). *Materials Research Proceeding* 2020; **16**, 6-15.

[64] AS Rini, A Fitrisia, Y Rati, L Umar and Y Soerbakti. Bio-colloidal silver nanoparticles prepared via green synthesis using sandoricum koetjape peel extract for selective colorimetry-based mercury ions detection. *Karbala International Journal of Modern Science* 2023; **9(2)**, 280-288.

[65] SD Chavan and DM Desai. Analytical method validation: A brief review. *World Journal of Advanced Research and Reviews* 2022; **16(2)**, 389-402.

[66] SM Ghurghure, MS Dyawarkonda and S Yanjane. Development and validation of UV-visible spectrophotometric method for estimation of tadalafil in bulk and formulation. *International Journal of Current Pharmaceutical Research* 2020; **12(3)**, 74-77.

[67] R Rina, M Baile and A Jain. A multifaceted review journal in the field of pharmacy a review: Analytical method development and validation. *Systematic Reviews in Pharmacy* 2021; **12(8)**, 450-454.

[68] F Dhanshri. A review on analytical method development. *International Journal of Creative Research Thoughts* 2022; **10(6)**, 840-854.

[69] MS Patil, RR Patil, SS Chalikwar, S Surana and S Firke. Analytical method development and validation: A review. *International Journal of Pharmaceutical and Biological Science Archive* 2019; **7(3)**, 70-81.

[70] V Swetha and Y Pooja. A review on analytical method development and validation. *World Journal of Pharmaceutical Research* 2020; **10(1)**, 745-768.

[71] S Zhang, H Xiong, L Zhou, W Ju, Z Yang, K Yan, B Yan and H Qu. Development and validation of in-line near-infrared spectroscopy based analytical method for commercial production of a botanical drug product. *Journal of Pharmaceutical and Biomedical Analysis* 2019; **174**, 674-682.

[72] B Marson, V Concentino, A Junkert, M Fachi, R Vilhena and R Pontarolo. Validation of analytical methods in a pharmaceutical quality system: An overview focused on HPLC methods. *Química Nova* 2020; **43(8)**, 1190-1203.